0026-895X/11/8006-1033–1046$25.00
MOLECULAR PHARMACOLOGY
Copyright © 2011 The American Society for Pharmacology and Experimental Therapeutics
Mol Pharmacol 80:1033–1046, 2011

Vol. 80, No. 6
74674/3729165
Printed in U.S.A.

Developing Chemical Genetic Approaches to Explore G Protein-Coupled Receptor Function: Validation of the Use of a Receptor Activated Solely by Synthetic Ligand (RASSL)

Elisa Alvarez-Curto, Rudi Prihandoko, Christofer S. Tautermann, Jurriaan M. Zwier, John D. Pediani, Martin J. Lohse, Carsten Hoffmann, Andrew B. Tobin, and Graeme Milligan

Molecular Pharmacology Group, Institute of Neuroscience and Psychology, College of Medical, Veterinary and Life Sciences, University of Glasgow, Glasgow, Scotland, United Kingdom (E.A.-C., J.D.P., G.M.); Department of Cell Physiology and Pharmacology, University of Leicester, Leicester England, United Kingdom (R.P., A.B.T.); Lead Identification and Optimization Support, Boehringer Ingelheim Pharma GmbH & Co. KG, Biberach, Germany (C.S.T.); Cisbio Bioassays, Codolet, France (J.M.Z.); and Department of Pharmacology and Toxicology, University of Wuerzburg, Wuerzburg, Germany (M.J.L., C.H.)

Received July 8, 2011; accepted August 30, 2011

ABSTRACT

Molecular evolution and chemical genetics have been applied to generate functional pairings of mutated G protein-coupled receptors (GPCRs) and nonendogenous ligands. These mutant receptors, referred to as receptors activated solely by synthetic ligands (RASSLs) or designer receptors exclusively activated by designer drugs (DREADDs), have huge potential to define physiological roles of GPCRs and to validate receptors in animal models as therapeutic targets to treat human disease. However, appreciation of ligand bias and functional selectivity of different ligands at the same receptor suggests that RASSLs may signal differently than wild-type receptors activated by endogenous agonists. We assessed this by generating forms of wild-type human M_3 muscarinic receptor and a RASSL variant that responds selectively to clozapine *N*-oxide. Although the RASSL receptor had reduced affinity for muscarinic antagonists, including atropine, stimulation with clozapine *N*-oxide produced effects very similar to those generated by acetylcholine at the wild-type M_3-receptor. Such effects included the relative movement of the third intracellular loop and C-terminal tail of intramolecular fluorescence resonance energy transfer sensors and the ability of the wild type and evolved mutant to regulate extracellular signal-regulated kinase 1/2 phosphorylation. Each form interacted similarly with β-arrestin 2 and was internalized from the cell surface in response to the appropriate ligand. Furthermore, the pattern of phosphorylation of specific serine residues within the evolved receptor in response to clozapine *N*-oxide was very similar to that produced by acetylcholine at the wild type. Such results provide confidence that, at least for the M_3 muscarinic receptor, results obtained after transgenic expression of this RASSL are likely to mirror the actions of acetylcholine at the wild type receptor.

Introduction

A number of G protein-coupled receptors (GPCRs) have been modified such that they become able to respond to a previously inert synthetic ligand, whereas, in parallel, they lose the ability to be activated by their native, endogenously produced ligand(s) (Conklin et al., 2008; Pei et al., 2008; Dong et al., 2010). Such modified receptors are described as either receptors activated solely by synthetic ligands (RASSLs) or as designer receptors exclusively activated by designer drugs (DREADDs) (Conklin et al., 2008; Pei et al., 2008; Dong et al., 2010). Such variants have been expressed transgenically to explore specific functions of the parent receptor when the synthetic ligand is provided (Redfern et al., 1999; Sweger et al., 2007; Alexander et al., 2009; Guettier et al., 2009). This approach has been of particular value in, for example, the

These studies were supported by the Biotechnology and Biosciences Research Council [Grant BB/E006302/1]; the Medical Research Council [Grant G0900050]; the Wellcome Trust [Grant 047600]; and a Biotechnology and Biosciences Research Council-Heptares Inc. studentship [Grant RM36G0146].
Article, publication date, and citation information can be found at http://molpharm.aspetjournals.org.
doi:10.1124/mol.111.074674.

ABBREVIATIONS: GPCR, G protein-coupled receptor; RASSL, receptor activated solely by synthetic ligand; DREADD, designer receptor exclusively activated by designer drug; hM_3, human muscarinic M_3; VSV, vesicular stomatitis virus; hM_3-R, human muscarinic M_3 receptor; FlAsH, fluorescein arsenical hairpin; IL3, third intracellular loop; FRET, fluorescence resonance energy transfer; DMEM, Dulbecco's modified Eagle's medium; PAGE, polyacrylamide gel electrophoresis; MOPS, 3-(*N*-morpholino)propanesulfonic acid; ERK, extracellular signal-regulated kinase; FBS, fetal bovine serum; BRET, bioluminescence resonance energy transfer; HEK, human embryonic kidney; Rluc, *Renilla reniformis* luciferase 8; HBSS, Hanks' balanced saline solution; EDT, ethanedithiol; DMSO, dimethyl sulfoxide; eCFP, enhanced cyan fluorescent protein; QNB, quinuclidinyl benzilate.

muscarinic acetylcholine receptors, where each of the five native muscarinic receptor subtypes responds to acetylcholine with similar potency (Wess, 2004; Armbruster et al., 2007; Wess et al., 2007; Nawaratne et al., 2008; Alexander et al., 2009; Guettier et al., 2009). Furthermore, identification of pharmacological agents that interact at a binding site that overlaps with that of acetylcholine but with high selectivity for an individual subtype has been difficult to achieve (Conn et al., 2009; Digby et al., 2010).

It is now widely appreciated that subtle modifications in agonist ligand structure can result in stabilization of distinct active states of a GPCR (Swaminath et al., 2005; Kobilka and Deupi, 2007; Bhattacharya et al., 2008). Such individual states can differentially modulate cellular signaling pathways (Swaminath et al., 2005; Kobilka and Deupi, 2007; Bhattacharya et al., 2008). Therefore, there must be a concern that use of a combination of a modified receptor and a distinct ligand might result in different outputs and thereby compromise the utility of such pairings to define details of function of the native receptor in vivo. There is already some evidence to favor this suggestion from studies performed on the serotonin 5-HT_4 receptor (Chang et al., 2007). This issue, however, has not been addressed previously in any detail. Using various forms of the wild-type human muscarinic M_3 receptor in parallel with equivalent RASSL forms of this receptor modified to respond to clozapine *N*-oxide rather than acetylcholine, we have explored potential differences at varying levels of receptor and cellular response. It is perhaps surprising that the pattern of regulation was very similar for the wild-type and RASSL forms, whether exploring initial conformational changes that occur upon ligand binding, interactions with β-arrestin 2, receptor internalization, ligand-induced phosphorylation of the ERK1/2 MAP kinases, or the extent and profile of phosphorylation of the receptor in response to appropriate agonists. This is despite a large reduction in affinity of the RASSL to bind the well characterized muscarinic receptor antagonist [^{3}H]QNB and the widely used antimuscarinic drug atropine. Molecular modeling provided a rationale for the selective activation of the RASSL variant by the selective ligand. These studies provide a strong indication that, at least for the M_3 receptor, this modified version is likely to allow production of meaningful and relevant information when expressed transgenically. Furthermore, they reinforce the use of designer receptors as valid and powerful tools to define and understand physiological responses in animal models.

Materials and Methods

Materials. Materials for cell culture were from Sigma-Aldrich (Gillingham, UK) or Invitrogen (Paisley, UK). Clozapine-*N*-oxide was from Enzo Life Sciences Ltd. (Exeter, UK). Other drugs used in this study were from Sigma-Aldrich. The various anti-muscarinic M_3-R antibodies and phosphoserine site-specific antisera have been described previously (Torrecilla et al., 2007; Poulin et al., 2010; Butcher et al., 2011). All secondary IgG horseradish peroxidase-linked antibodies were from GE Healthcare (Chalfont St. Giles, Buckinghamshire, UK). The radioligand [^{3}H]QNB was from PerkinElmer Life and Analytical Sciences (Waltham, MA). All oligonucleotides were purchased from Thermo Fisher Scientific (Ulm, Germany). Flp-In T-REx 293 cells were from Invitrogen. Tag-lite reagents and SNAP-tag reagents were supplied by Cisbio Bioassays (Bagnols sur Ceze, France) and New England Biolabs (Hitchin, UK).

Molecular Constructs. Generation of the human muscarinic M_3 (hM_3)-RASSL by site-directed mutagenesis and VSV-G-SNAP-hM_3-R and VSV-G-SNAP-hM_3-RASSL constructs was described previously (Alvarez-Curto et al., 2010). The hM_3-R intramolecular FRET-sensor construct was generated as described in Ziegler et al. (2011). In brief, the short amino acid motif CCPGCC, which specifically defines the fluorescein arsenical hairpin binder (FlAsH) sequence was introduced as replacement of amino acids 271 to 465 in the third intracellular loop (IL3) of the hM_3-R. The modified receptor was then fused in-frame to enhanced cyan fluorescent protein (eCFP; BD Bioscience Clontech, Heidelberg, Germany). All resulting constructs were cloned into either pcDNA3 or pcDNA5/FRT/TO (Invitrogen) and confirmed by sequencing. The equivalent hM_3-RASSL intramolecular FRET-sensors introduced either or both cysteine (C) for tyrosine (Y) at residue 149 (position 3.33 in the nomenclature of Ballesteros and Weinstein (1995)) and glycine (G) for alanine (A) at residue 239 (position 5.46) as described previously (Armbruster et al., 2007).

Generation of Stable Flp-In T-REx 293 Cells. Cells were maintained in Dulbecco's modified Eagle's medium (DMEM) without sodium pyruvate, 4500 mg/l glucose, and L-glutamine, supplemented with 10% (v/v) fetal calf serum, 1% penicillin/streptomycin mixture, and 10 μg/ml blasticidin in a humidified atmosphere. To generate Flp-In T-REx 293 cells able to inducibly express the different cDNA constructs, cells were transfected with a 1:9 mixture of cDNA in pcDNA5/FRT/TO vector and the pOG44 vector (Invitrogen) using Effectene (QIAGEN, West Sussex, UK), according to the manufacturer's instructions and as described previously (Ellis et al., 2006; Stoddart et al., 2008; Smith et al., 2009; Ward et al., 2011). After 48 h, the medium was changed to medium supplemented with 200 μg/ml hygromycin B (Roche Diagnostics, Mannheim, Germany) to initiate selection of stably transfected cells.

Cell Membrane Preparation. Pellets of cells were frozen at −80°C for a minimum of 1 h, thawed, and resuspended in ice-cold 10 mM Tris, 0.1 mM EDTA, pH 7.4 (Tris-EDTA buffer) supplemented with Complete protease inhibitors cocktail (Roche Diagnostics). Cells were homogenized on ice by 40 strokes of a glass-on-Teflon homogenizer followed by centrifugation at 1000*g* for 5 min at 4°C to remove unbroken cells and nuclei. The supernatant fraction was removed and passed through a 25-gauge needle 10 times before being transferred to ultracentrifuge tubes and subjected to centrifugation at 50,000*g* for 45 min at 4°C. The resulting pellets were resuspended in ice-cold Tris-EDTA buffer. Protein concentration was assessed and membranes were stored at −80°C until required.

Radioligand Binding Assays. Saturation binding isotherms were established after the addition of 1 μg (hM_3-R) or 10 μg (hM_3-RASSL) of membrane protein to assay buffer (20 mM HEPES, 100 mM NaCl, and 10 mM $MgCl_2$, pH 7.4) containing varying concentrations of [^{3}H]QNB (50.5 Ci/mmol). Nonspecific binding was determined in the presence of 10 μM atropine. Reactions were incubated for 90 min at 30°C, and bound ligand was separated from free by vacuum filtration through GF/C filters (Brandel Inc., Gaithersburg, MD). The filters were washed twice with assay buffer, and bound ligand was estimated by liquid scintillation counting.

Cell Lysates and Western Blotting. Cells were washed once in cold phosphate-buffered saline and harvested with ice-cold radioimmunoprecipitation assay buffer (50 mM HEPES, 150 mM NaCl, 1% Triton X-100, 0.5% sodium deoxycholate, 10 mM NaF, 5 mM EDTA, 10 mM NaH_2PO_4, and 5% ethylene glycol, pH 7.4) supplemented with Complete protease inhibitor cocktail (Roche Diagnostics). Extracts were passed through a 25-gauge needle and incubated for 15 min at 4°C while spinning on a rotating wheel. Cellular extracts were then centrifuged for 30 min at 14,000*g*, and the supernatant was recovered. Samples were heated at 65°C for 15 min and subjected to SDS-PAGE analysis using 4 to 12% Bis-Tris gels (NuPAGE; Invitrogen) and MOPS buffer. Proteins were then electrophoretically transferred onto nitrocellulose membranes that were blocked for 45 min in 5% fat-free milk in 1× Tris-buffered saline containing 0.1%

(v/v) Tween 20 and subsequently incubated with the required primary antibody overnight at 4°C. Incubation with the appropriate horseradish peroxidase-linked IgG secondary antiserum was performed for 2 h at room temperature. Immunoblots were developed by application of enhanced chemiluminescence solution (Thermo Fisher Scientific).

ERK1/2 Phosphorylation Assays. ERK1/2 phosphorylation assays were performed using the AlphaScreen Surefire kit (Perkin-Elmer Life and Analytical Sciences). Cells were plated on 96-well poly-D-lysine-coated plates (4×10^4 cells/well), and receptor construct expression induced the next day with either varying concentrations or 5 ng/ml doxycycline. In experiments in which pertussis toxin was used, 25 ng/ml was added simultaneously with the doxycycline and incubated for 16 to 18 h. Before ligand stimulation, cells were serum-starved for 5 h in growth medium lacking FBS. Stimulation of cells was terminated by rapid aspiration of the medium and fast addition of 50 μl of 1× lysis buffer that is provided with the kit. Lysates were subsequently processed according to the manufacturer's instructions.

$[Ca^{2+}]_i$ Mobilization Assays. Cells induced to express forms of either hM_3-R or hM_3-RASSL were plated in black, clear-bottomed 96-well plates (Greiner Bio-One GmbH, Frickenhausen, Germany) and induced with 5 ng/ml doxycycline for 24 h. Cells were incubated at 37°C in the dark with the Ca^{2+}-sensitive dye Fura-2 diluted to 3 μM in DMEM for 30 min, subsequently washed twice with HEPES physiological saline solution (130 mM NaCl, 5 mM KCl, 1 mM $CaCl_2$, 1 mM $MgCl_2$, 20 mM HEPES, and 10 mM D-glucose, pH 7.4) and transferred to a FlexStation II (Molecular Devices, Sunnyvale, CA), where they were treated with ligands. Alteration of intracellular calcium was recorded as changes of Fura-2 340/380-nm emission ratio.

Tag-Lite Internalization Assays. Cells were plated on black, poly-D-lysine-coated 96-well plates (10^5 cells/well), and induced with 5 ng/ml doxycycline for 24 h. The next day, the plate was cooled on ice for 5 min, and cells were labeled with 100 nM SNAP-Lumi4Tb for 1 h at 4°C. Cells were washed four times with cold labeling medium (Cisbio Bioassays), after which ligands and Tag-lite internalization buffer were added. Plates were then read at different time intervals in a PheraStar FS plate reader (BMG Labtech, Offenburg, Germany), monitoring the changes of donor emission at 620 nm (integration start, 1500 μs; integration time, 1500 μs) and acceptor emission at 520 nm (integration start, 150 μs; integration time, 400 μs). The ratio was finally calculated as (donor/acceptor channel) $\times 10^4$.

***β*-arrestin-2 BRET Assays.** HEK293T cells were transfected with the required receptor, C-terminally tagged with mCitrine, and β-arrestin-2, C-terminally tagged with *Renilla reniformis* luciferase 8 (Rluc) (ratio 4:1), using polyethylenimine (Jenkins et al., 2010, 2011). An additional transfection was performed with only the Rluc construct and empty expression vector pcDNA3. From 10-cm dishes, cells were seeded at 5×10^4 cells per well into poly-D-lysine-coated white 96-well plates. After 24 h, cells were washed twice with Hanks' balanced salt solution (HBSS), pH 7.4, and coelenterazine-h (Promega, Southampton, UK) was added to a final concentration of 5 μM. Cells were incubated in darkness for 10 min at 37°C before addition of ligands, after which they were incubated for a further 10 min at 37°C before reading on a PheraStar FS plate reader, which allows simultaneous reading of emission signals detected at 475 and 535 nm. Net bioluminescence resonance energy transfer (BRET) values were defined as the 535 nm/475 nm ratio of cells coexpressing Rluc and mCitrine minus the BRET ratio of cells expressing only the Rluc construct in the same experiment. This value was multiplied by 1000 to obtain mBRET units.

Epifluorescence Imaging of SNAP-tag Proteins in Live Cells. Cells induced to express the receptor construct of interest were grown on coverslips pretreated with 0.1 mg/ml poly-D-lysine. SNAP-tag–specific substrates were diluted in complete DMEM from a stock solution yielding a labeling solution of 5 μM dye substrate. The medium on the cells expressing a SNAP-tag fusion protein was replaced with the labeling solution and incubated at 37°C, 5% CO_2 for 30 min. Cells were washed three times with complete medium and a further time with HEPES physiological saline solution (130 mM NaCl, 5 mM KCl, 1 mM $CaCl_2$, 1 mM $MgCl_2$, 20 mM HEPES, and 10 mM D-glucose, pH 7.4). Coverslips were then transferred to a microscope chamber, where they were imaged using an inverted Nikon TE2000-E microscope (Nikon Instruments, Melville, NY) equipped with a 40× (1.3 numerical aperture) oil-immersion Pan Fluor lens and a cooled digital photometrics Cool Snap-HQ charge-coupled device camera (Roper Scientific, Trenton, NJ).

FlAsH Labeling. Cells were grown on poly-D-lysine-treated glass coverslips (number 0) and induced to express the construct of interest with doxycycline for 24 h. The next day, the coverslips bearing induced cells were transferred to six-well multiplates containing 2 ml of control phenol red-free HBSS, 1× supplemented with 10 mM glucose (Invitrogen). Each well was washed three times (10 min per wash) with control HBSS. After the final wash, the HBSS solution was aspirated from each well and replaced with 1.8 ml of control HBSS. In between washes, HBSS containing 1 μM FIAsH and 12.5 μM ethanedithiol (EDT) was prepared fresh as follows: 25 mM EDT DMSO solution was freshly prepared in a 2-ml Eppendorf tube by adding 2.1 μl of EDT to 1 ml of DMSO and then vortex mixing. This mixture was at room temperature for 20 min to ensure complete conversion of FIAsH to its FIAsH-EDT2 form. FIAsH labeling solution (1 μM; for six coverslip samples) was made by first adding 6 μl of 2 mM Lumio Green stock solution (Invitrogen) to a new 2-ml Eppendorf tube; 6 μl of 25 mM EDT was then added to this solution, mixed, and left in the dark at room temperature for 20 min.

After 20 min, 1.2 ml of control HBSS solution containing 10 mM glucose was added to this tube and vortex-mixed. This EDT/FIAsH/HBSS solution was then allowed to stand for 20 min in the dark to ensure complete binding of EDT. After 20 min, 200-μl amounts of the EDT/FIAsH/HBSS solution were added to each well containing 1.8 ml of control HBSS. The six-well multiplate was then gently swirled to ensure uniform distribution of the labeling solution. Cells were then incubated at 37°C for 1 h in the dark with the FlAsH suspended HBSS solution containing 12.5 μM EDT. During this incubation period, EDT/HBSS washing solution was prepared by mixing 42 μl of EDT with 1 ml of DMSO in a 1.5-ml Eppendorf tube (500 mM EDT in DMSO). Twenty-five microliters of this mixture was added to 50 ml of control HBSS and mixed to form a final HBSS/glucose solution containing 250 μM EDT. After 1 h, the cells were removed from the incubator, and the FlAsH labeling solution was then aspirated from each well and replaced with 3 ml of EDT/HBSS wash solution. Cells were incubated for 15 min in the dark to reduce nonspecifically bound FlAsH. This washing procedure was repeated twice more to further reduce background staining. Cells were then rinsed three times (5 min/wash), with FlAsH-free control HBSS solution to ensure complete removal of EDT from labeled cells. Labeled cells were then stored at room temperature in the dark before intramolecular fluorescence resonance energy transfer (FRET) imaging experimentation.

Intramolecular eCFP-FlAsH FRET Experiments. Washed FlAsH-labeled cells were placed into a microscope chamber containing physiological HEPES-buffered saline solution (130 mM NaCl, 5 mM KCl, 1 mM $CaCl_2$, 1 mM $MgCl_2$, 20 mM HEPES, and 10 mM D-glucose, pH 7.4). Cells were then imaged using an inverted Nikon TE2000-E microscope (Nikon Instruments) equipped with a 40× (1.3 numerical aperture) oil immersion Fluor lens. Excitation light was generated from a computer-controlled Optoscan monochromator (Cairn Research, Faversham, UK), which was coupled to an ultra-highpoint intensity Optosource lamp (Cairn Research), fitted with a 103-W mercury arc lamp (Osram 103W/2). Monochromator was set to 427 nm/5 nm band width or 504 nm/5 nm band width, to visualize surface located eCFP-tagged receptors labeled with FlAsH. Excitation light (427 or 504 nm) was reflected through the Fluor objective lens using a cyan/yellow fluorescent protein dual band dichroic filter (Semrock; Rochester, NY), mounted in the microscope. FRET and

donor emission images were recorded exactly at the same time interval using a Quadview 2 image splitting device (Photometrics, UK), coupled to a CoolSnap-HQ2 camera connected to the microscope's bottom port for maximal detection of emitted fluorescence. FRET and donor signals were detected simultaneously using the following Chroma (Brattleboro, VT) ET series dichroic and emitters mounted in the Quadview 2 cube: ET t505LPXR dichroic, ET535/30 nm, ET 470/30 nm.

Using the streaming capability of the multiple dimensional wavelength acquisition module of MetaMorph (ver. 7.7.4; Molecular Devices), ligand-induced changes in intramolecular FRET during excitation with 427 nm light were recorded at 40-ms intervals directly to the computer's hard drive. The Cool Snap-HQ2 camera was operated in 14-bit mode, and exposure time, binning (8 × 8), and camera gain were kept constant for all streaming experiments. Computer control of all electronic hardware and camera streaming acquisition was achieved using MetaMorph software. Transistor-transistor logic–controlled solenoid valves connected to a peristaltic pump operated at a flow rate of 5 ml/min were used to rapidly add or remove test ligand drugs into the imaging chamber.

Intramolecular FRET Ratio Quantification. Using MetaMorph's split view module, saved images were split to form individual FRET or donor stream time-lapse stacks. Each stack was corrected for background fluorescence and exported into MetaMorph's align module to ensure there was no x or y pixel shift misalignment between the donor and FRET channel stream stacks before the calculation of the intramolecular FRET ratio. Intramolecular FRET values were measured by manually drawing regions of interest around the profile of individual cells and averaging the signals within the delimited regions of interest for each time-lapse image collected at 470 or 535 nm emission. Ratiometric FRET values were then calculated as the average 535 nm emission intensity divided by the average 470 nm emission intensity. Quantified ratio values were exported into Prism 5.02 (GraphPad Software Inc., San Diego, CA) and using GraphPad's transforming module set to a value of 1.0 at the onset of each experiment and plotted over time.

[^{32}P]Orthophosphate Labeling and hM$_3$ Receptor Immunoprecipitation. Cells grown on six-well plates at ~90% confluence were washed three times in 1 ml of phosphate free Krebs/HEPES buffer (10 mM HEPES, 118 mM NaCl, 4.69 mM KCl, 1.18 mM $MgSO_4 \cdot 7H_2O$, 1.3 mM $CaCl_2$, 25.0 mM $NaHCO_3$, and 11.7 mM glucose, pH 7.4) and then incubated with 50 μCi/ml [^{32}P]orthophosphate (185 MBq; PerkinElmer Life and Analytical Sciences) for 1 h at 37°C. Cells were stimulated with the appropriate agonist for 5 min at 37°C. The reactions were terminated by rapid aspiration of the buffer followed by addition of 1 ml of ice-cold radioimmunoprecipitation assay buffer (10 mM Tris, 160 mM NaCl, 2 mM EDTA, 20 mM glycerol-2-phosphate, 1% Nonidet P-40, and 0.5% sodium deoxycholate, pH 7.4) for 10 min on ice. Cell lysates were cleared by centrifugation (20,000g for 5 min), and receptors were immunoprecipitated from precleared lysates using 2 μg/sample of in-house polyclonal anti-M$_3$-R antibody. Immunocomplexes were isolated on protein A-Sepharose beads (1.5 g; Thermo Fisher Scientific), and the beads were washed three times with ice-cold buffer (10 mM Tris, 2 mM EDTA, and 20 mM glycerol-2-phosphate, pH 7.4). Immunocomplexes were resuspended in 2× SDS-PAGE sample buffer (125 mM Tris, 200 mM dithiothreitol, 4% SDS, 20% glycerol, and 0.05% bromphenol blue, pH 6.8) and placed in a 60°C water bath for 3 to 5 min. Receptor proteins were resolved on 8% SDS-PAGE gels and electroblotted onto nitrocellulose membranes using the semidry transfer method (Bio-Rad Laboratories, Hercules, CA) and Tris-glycine transfer buffer (25 mM Tris, 190 mM glycine, and 20% methanol). Receptor phosphorylation was detected by autoradiography.

Tryptic Digestion and Two-Dimensional Electrophoresis. Nitrocellulose membrane containing the receptor of interest was excised and incubated with 200 μl of blocking solution (0.5% polyvinylpyrrolidone containing 0.6% acetic acid) for 30 min at 37°C. Membrane pieces were washed three times with distilled water and one time with 50 mM ammonium bicarbonate. Proteins on the membrane pieces were digested with 10 μg/ml trypsin (Promega) diluted in 50 mM ammonium bicarbonate solution overnight at 37°C (final volume, 60 μl). The supernatant from the tryptic digest was recovered and transferred to fresh tubes. The membrane pieces were washed three times with 50 to 100 μl of distilled water. The supernatant from each wash was pooled and dried using a SpeedVac (Thermo Fisher Scientific) at room temperature for 2 to 6 h. The pellet was dissolved in 25 to 50 μl of pH 1.9 buffer [88% formic acid/acetic acid/water, 25:78:897 (v/v/v)] and dried again using the SpeedVac centrifuge. The pellet was resuspended in 5 to 10 μl of pH 1.9 buffer, vortex-mixed intensely, and applied to a cellulose thin-layer chromatography plate in small volumes (≤1 μl). Samples were dried with a fan without heating and separated in two dimensions. The first dimension was electrophoresis in pH 1.9 buffer for 30 to 40 min at 2000 V using the HTLE 7002 electrophoresis system. The second dimension was ascending thin-layer chromatography using isobutyric acid chromatography buffer [isobutyric acid/n-butanol/pyridine/acetic acid/water, 1250:38:96:58:558 (v/v)]. The plate was dried extensively in a fume hood, wrapped in cling film, and exposed to a PhosphorImager. Resolved phosphopeptides were visualized using the STORM PhosphorImager instrument (GE Healthcare) and quantified using alphaimager software (Alpha Innotech, San Leandro, CA).

Results

Analysis of Ligand-Induced Conformational Changes in hM$_3$ Intramolecular FRET Sensors. Detailed analysis of the effects of ligands on rapid changes in conformation or activation state(s) of GPCRs can be performed using intramolecular FRET sensors (Hoffmann et al., 2005; Zürn et al., 2009). In initial studies, in HEK293T cells, we expressed transiently a form of the hM$_3$-R containing a FlAsH tag inserted into IL3 and with eCFP linked in-frame to the C-terminal tail. To optimize the FRET response, we deleted a segment (amino acids 271–465) from IL3 (Ziegler et al., 2011). Once the FlAsH tag had been labeled with the FRET acceptor Lumio Green, this construct generated a rapid increase in the basal FRET signal upon addition of carbachol but not clozapine N-oxide (Fig. 1A). We then introduced Y149C and/or A239G mutations into this construct, both individually and in combination, and repeated the studies. The sensor containing only the Y149C mutation responded to neither carbachol nor clozapine N-oxide (Fig. 1B), whereas the sensor containing only the A239G mutation responded to carbachol (1 mM), although with slower kinetics than the hM$_3$-R sensor, but failed to respond to clozapine N-oxide (Fig. 1C). After introduction of both the Y149C and A239G alterations into the receptor sequence, the sensor did not respond to carbachol at concentrations up to 1 mM but did respond to clozapine N-oxide, with a significantly larger response to 100 μM than to 10 μM of this ligand (Fig. 1D). As such, it behaved as an hM$_3$-RASSL FRET sensor.

Based on these initial studies, Flp-In T-REx 293 cell lines able to express either the hM$_3$-R or the hM$_3$-RASSL FRET sensor were generated. Here, receptor expression is under the control of a doxycycline-inducible promoter. Saturation binding studies performed on membranes generated from cells induced to express the hM$_3$-R sensor showed this construct to have high affinity [K_D = 75 ± 28 pM (mean ± S.E.M.), n = 3] for [^{3}H]QNB (Fig. 2A), whereas the hM$_3$-RASSL sensor displayed some 100 fold lower affinity for this ligand (K_D = 7.9 ± 2.2 nM, n = 3) (Fig. 2B), a feature that presumably reflects alteration of the amino acids used to

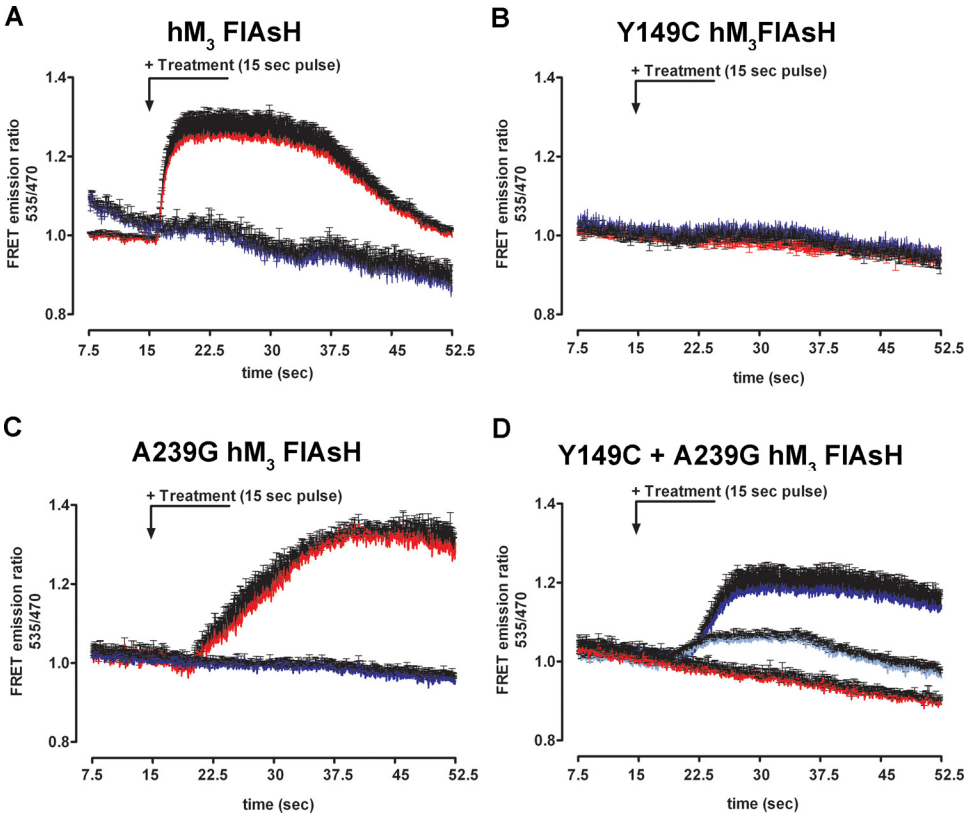

Fig. 1. Ligand regulation of intramolecular hM_3 FRET sensor variants: from hM_3-R to hM_3-RASSL. HEK293T cells were transfected transiently to express FlAsH-eCFP FRET sensors: hM_3 FlAsH (A), Y149C hM_3 FlAsH (B), A239G hM_3 FlAsH (C), or Y149C + A239G hM_3 FlAsH (RASSL) (D). These were exposed for 15 s (see bar) to 1 mM carbachol (red trace) or either 100 μM (blue trace) or 10 μM (light blue trace) (only in D) clozapine *N*-oxide. Traces represent mean ± S.E.M. from 10 to 15 individual cells.

create the RASSL within the ligand-binding pocket of the hM_3-R (see *Discussion*). Because atropine is frequently used as a standard muscarinic antagonist and was used to define nonspecific binding of [^{3}H]QNB in these studies, we also assessed the affinity of this ligand at these two forms of the hM_3 receptor via competition binding studies. Atropine also displayed reduced affinity at the hM_3-RASSL sensor (estimated K_i = 47 ± 17 nM) compared with the equivalent hM_3-R (estimated K_i = 0.74 ± 0.1 nM).

We next assessed the functionality of the expressed constructs in calcium mobilization assays. Despite the multiple molecular modifications introduced into the receptors, each was able to respond robustly to the appropriate agonists, with potency for carbachol and acetylcholine in the case of the hM_3-R construct (pEC_{50} = 7.2 ± 0.04 and 7.8 ± 0.3, n = 3, respectively) and to clozapine *N*-oxide at the hM_3-RASSL (pEC_{50} = 7.6 ± 0.1, n = 3) (Fig. 2C; Table 1).

After addition of the FlAsH labeling reagent Lumio Green to cells induced to express either of the intramolecular FRET sensors (Fig. 3A) and subsequent washout, imaging of these cells showed the FlAsH sequence to be labeled effectively (Fig. 3B). Parallel imaging also identified the presence of the eCFP tag at the surface of the cells (Fig. 3B). FRET imaging of cells induced to express the hM_3-R FRET sensor demonstrated a rapid increase in FRET signal upon addition of acetylcholine but not in response to either clozapine *N*-oxide or atropine (not shown). Carbachol also induced a rapid and concentration-dependent increase in FRET (Fig. 3C, left) [pD_2 (pEC_{50}) = 4.9 ± 0.2, n = 5] (Table 1). In cells expressing the hM_3-RASSL sensor clozapine *N*-oxide (pD_2 = 5.1 ± 0.4, n = 4) (Fig. 3D), but not carbachol or atropine, produced a similar increase in FRET.

Generation of VSV-G and SNAP-Tagged hM_3 Constructs. To further compare the functional properties of hM_3-R and hM_3-RASSL, these forms of the receptor were tagged at the N terminus with an anti-VSV-G epitope tag and the 20-kDa SNAP-tag sequence (Alvarez-Curto et al., 2010). These forms were also expressed stably in Flp-In T-REx 293 cell lines. After induction with doxycycline, addition of SNAP-488, a cell-impermeant, SNAP-tag–specific substrate, allowed visual detection of cell surface-delivered forms of the receptors in intact cells (Fig. 4B), because this substrate can link covalently to proteins that incorporate the SNAP-tag (Gautier et al., 2008; Alvarez-Curto et al., 2010; Ward et al., 2011). Receptor expression was confirmed and quantified firstly by performing saturation specific [^{3}H]QNB binding studies on membranes from cells treated with or without doxycycline. In cells induced to express VSV-G-SNAP hM_3-R [^{3}H]QNB bound with high affinity (K_D = 35 ± 9 pM) (Fig. 4C). By contrast, in the absence of doxycycline, little specific [^{3}H]QNB binding was detected (not shown). As noted previously (Alvarez-Curto et al., 2010), after induction of expression of VSV-G-SNAP hM_3-RASSL, [^{3}H]QNB bound with appreciably lower affinity (K_D = 1.4 ± 0.04 nM) (Fig. 4D). Atropine also displayed lower affinity at this RASSL variant than at the equivalent hM_3-R construct. Correction for receptor occupancy of measured IC_{50} values produced affinity estimates for atropine of 0.74 ± 0.2 nM (n = 3) for VSV-G-SNAP hM_3-R and 23 ±1.4 nM (n = 3) for VSV-G-SNAP hM_3-RASSL. The need to use high concentrations of [^{3}H]QNB to approach a binding saturation isotherm for VSV-G-SNAP hM_3-RASSL resulted in relatively poor specific to total binding values for [^{3}H]QNB. Expression of the two forms of the hM_3 receptor at the surface of cells was therefore

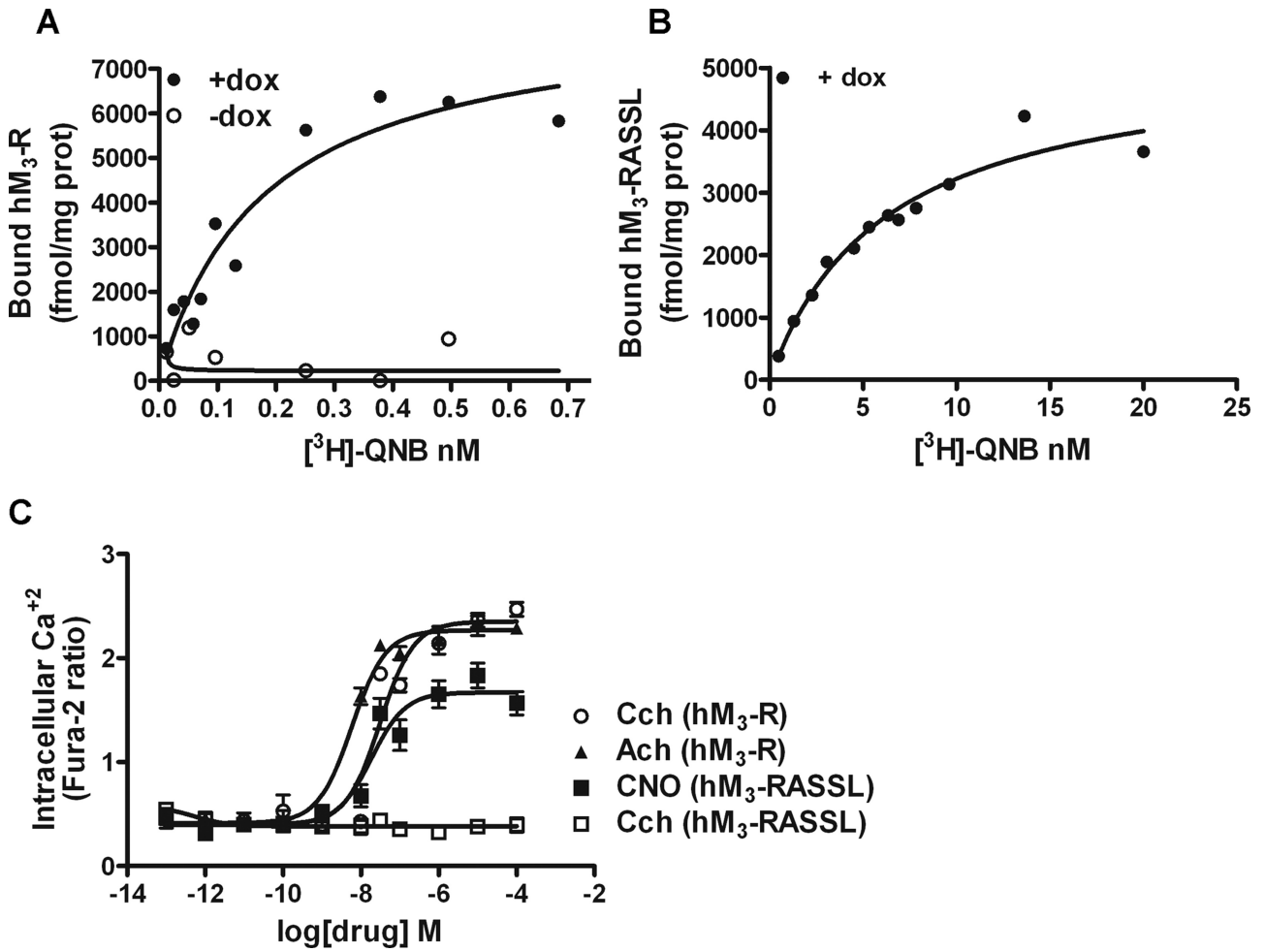

Fig. 2. Expression and function of intramolecular FRET sensor forms of the hM_3 receptor. Membranes were prepared from untreated cells (− dox) harboring hM_3-R (A) or hM_3 RASSL (B) intramolecular FRET sensors or those induced (+ dox) to express the constructs. These were used to measure the specific binding of varying concentration of [^{3}H]QNB. Two further experiments produced similar results. C, calcium mobilization in response to varying concentrations of acetylcholine (Ach) and carbachol (Cch) at the hM_3-R and to clozapine *N*-oxide (CNO) and Cch at the hM_3-RASSL is shown. Data represent means ± S.E.M. of triplicate assays from a single experiment. Two further experiments produced similar results.

further assessed via the binding to intact cells and associated luminescence intensity at 620 nm of a single concentration (20 nM) of SNAP-lumi4Tb. This is also able to bind covalently to the SNAP-tag present in the extracellular N-terminal domain of the constructs (Alvarez-Curto et al., 2010; Ward et al., 2011). Given the location of the SNAP-tag, this should be insensitive to the alterations in the [^{3}H]QNB binding pocket used to produce the hM_3-RASSL (Fig. 4E). Virtually no binding of SNAP-lumi4Tb to either set of cells was noted in the absence of doxycycline, but this increased, over a range 1 to 10 ng/ml, the antibiotic, because expression of the corresponding receptor was induced and was similar in the two cell lines (Fig. 4E).

Analysis of ERK1/2 Responses of the hM_3-R and hM_3-RASSL. There is currently great interest in the concept that different agonist ligands may selectively stabilize distinct conformations of a GPCR and thus potentially produce distinct signals or different patterns of regulation. This is generally referred to as "functional selectivity" or "ligand bias" (Mailman, 2007; Violin and Lefkowitz, 2007; Vaidehi and Kenakin, 2010; Rajagupal et al., 2010; Kenakin, 2011; Smith et al., 2011). The evolution of distinct molecular pairs of designer ligands and receptors makes assessment of the detailed function of such pairings of key importance before they can be employed widely, because there is no a priori reason to believe that they should function in an equivalent manner. We therefore compared the effects of the endogenous agonist acetylcholine and its stable analog carbachol at the hM_3-R construct with those of clozapine *N*-oxide at the hM_3-RASSL. Cells induced to express VSV-G-SNAP hM_3-R or VSV-G-SNAP hM_3-RASSL by treatment with 5 ng/ml doxycycline were challenged with various concentrations of acetylcholine, carbachol, or clozapine *N*-oxide for 5 min, and phospho-ERK1/2 levels were subsequently measured. In cells induced to express VSV-G-SNAP hM_3-R, both acetylcholine and carbachol produced robust, concentration-dependent increases (Fig. 5A; Table 1), acetylcholine being approximately 10-fold more potent than carbachol: pEC_{50} = 7.9 ± 0.3 (n = 2) and 6.9 ± 0.1 (n = 3), respectively. By contrast, even at 100 μM, clozapine *N*-oxide was without effect (Fig. 5A). The reverse was observed in cells induced to express VSV-G-SNAP hM_3-RASSL. Little or no response to carbachol or acetylcholine was observed at concentrations up to 100 μM, whereas clozapine *N*-oxide produced a robust, concentration-dependent

TABLE 1

Comparisons of ligand affinity/potency at hM_3-R and hM_3-RASSL constructs

All experiments were performed on stable Flp-In T-REx 293 cell lines able to express the noted construct upon addition of doxycycline. Data shown are the mean ± S.E.M. of two to four independent experiments performed in triplicate (see text and figure legends for full details). B_{max} values were obtained from cells induced to express the receptors with a maximally effective concentration of doxycycline.

	K_D [^{3}H]QNB	B_{max}	K_i Atropine	pEC_{50}									
				FRET		$[Ca^{2+}]$		pERK1/2			Internalization		
				Cch	CNO	Cch	CNO	Ach	Cch	CNO	Ach	Cch	CNO
		pmol/mg	*nM*										
hM_3-R FlAsH	75 ± 28 pM	6.5 ± 0.66	0.74 ± 0.1	4.9 ± 0.2	>3.0	7.2 ± 0.04		7.8 ± 0.3		N.D.			N.A.
hM_3-RASSL FlAsH	7.9 ± 2.2 nM	3.5 ± 0.89	47 ± 17	>3.0	5.1 ± 0.4		7.6 ± 0.1			N.D.			N.A.
VSV-SNAP-hM_3-R	35 ± 9 pM	12.6 ± 1.2	0.74 ± 0.2	N.A.		7.5 ± 0.4			6.9 ± 0.1	>4.0	7.9 ± 0.3	4.8 ± 0.16	
VSV-SNAP-hM_3-RASSL	1.4 ± 0.04 nM	2.6 ± 013	23 ± 1.4	N.A.		7.7 ± 0.6			>4.0	7.6 ± 0.4			6.2 ± 0.15

Ach, acetylcholine; Cch, carbachol; CNO, clozapine *N*-oxide, N.D., not determined; N.A., not applicable.

increase in phospho-ERK1/2 with pEC_{50} = 7.6 ± 0.4 (n = 3) (Fig. 5B; Table 1). It is noteworthy that clozapine *N*-oxide did not seem to bind VSV-G-SNAP hM_3-R with significant affinity and potentially act as an antagonist, because even in the presence of 100 μM clozapine *N*-oxide, the concentration-response curve to carbachol was little affected (Fig. 5C). Likewise, 100 μM carbachol was unable to alter the concentration-response curve to clozapine *N*-oxide at VSV-G-SNAP hM_3-RASSL (Fig. 5D). Subsequently, we assessed the kinetics of ERK1/2 phosphorylation in response to ligands in these cells. In cells induced to express VSV-G-SNAP hM_3-R, both carbachol and acetylcholine promoted rapid and high-level generation of phospho-ERK1/2 (Fig. 6A), and this was sustained over the course of at least 60 min (Fig. 6A). By contrast, fetal bovine serum [20% (v/v)] used as a positive control did not result in sustained ERK1/2 phosphorylation, although it did produce a peak of phospho-ERK1/2 within 5 min that rapidly decayed back to basal levels (Fig. 6A). Neither atropine nor clozapine *N*-oxide promoted ERK1/2 phosphorylation at any time point measured. In VSV-G-SNAP hM_3-RASSL-expressing cells treatment with clozapine *N*-oxide also resulted in sustained activation of ERK1/2 (Fig. 6B), whereas, again, FBS produced a more modest response that was transient in nature (Fig. 6B). In these cells, both carbachol and acetylcholine (at 100 μM) caused a modest increase in ERK1/2 phosphorylation, but in both theses cases, the signal was as transitory as observed for FBS (Fig. 6B).

Analysis of Receptor Internalization and Interaction with β-Arrestin-2. We next quantified the extent of receptor internalization in response to ligand challenge for 40 min by monitoring changes in FRET between the lumi4-Tb labeled receptor and Tag-lite internalization buffer. VSV-G-SNAP-tagged hM_3-R and hM_3-RASSL-expressing cells were labeled with 100 nM SNAP-lumi4-Tb, the luminescent probe, and subsequently incubated with a mixture of Tag-lite internalization reagent and receptor ligands (Fig. 7, A and B). At zero time, cell surface expression of each variant was detected. Internalization of the receptor variants after treatment of the cells with ligands was concentration-dependent with pEC_{50} = 4.8 ± 0.16 for carbachol at the hM_3-R (Fig. 7A; Table 1) and pEC_{50} = 6.2 ± 0.15 for clozapine *N*-oxide at the hM_3-RASSL (Fig. 7A; Table 1). In contrast, and as expected, the antagonist atropine (10 μM) elicited no detectable internalization of either receptor construct (not shown). Because receptor internalization is often preceded by interactions with a β-arrestin, we also assessed the potential interaction of both hM_3-R and hM_3-RASSL forms with β-arrestin-2. HEK293T cells were transiently cotransfected with β-arrestin-2-RLuc and either Flag-hM_3-R-Citrine (Alvarez-Curto et al., 2010) or a similar construct containing the RASSL variant but with an N-terminal c-Myc tag. Addition of coelenterazine-h to such cells resulted in BRET that was produced in a concentration-dependent manner by both acetylcholine and carbachol in cells expressing Flag-hM_3-R-Citrine, and with similar potencies (carbachol pEC_{50} = 4.4 ± 0.5, n = 4; acetylcholine pEC_{50} = 4.6 ± 0.4, n = 4) (Fig. 7C). No such effect was produced by clozapine *N*-oxide (Fig. 7C). By contrast, in cells expressing c-Myc-hM_3-RASSL-Citrine, clozapine *N*-oxide potently enhanced BRET signals (pEC_{50} = 6.4 ± 0.3, n = 3), whereas acetylcholine and carbachol produced no significant effects at concentrations up to 1 mM (Fig. 7D).

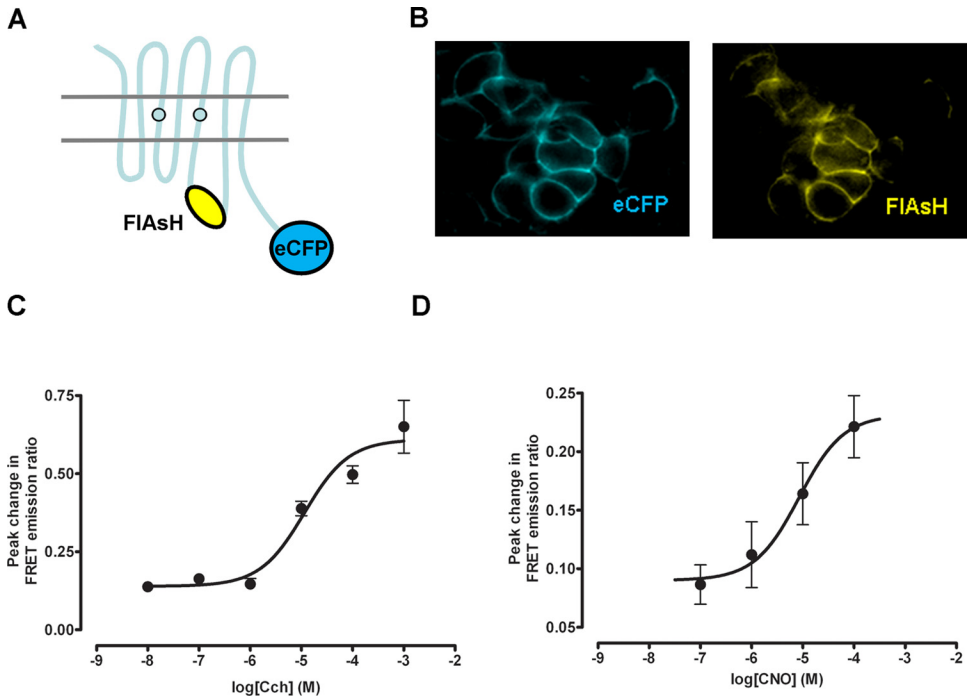

Fig. 3. Appropriate agonists selectively modulate intramolecular FRET sensor forms of the hM_3. A, diagram of the hM_3-R intramolecular FRET sensors shows the relative positioning of the introduced FlAsH sequence and the appended eCFP. Circles represent the amino acids mutated to generate the RASSL variant. B, cells induced to express the hM_3-R FRET sensor were labeled with Lumio Green and imaged (FlAsH) or imaged to detect eCFP. Expression of the hM_3-R (C) or hM_3-RASSL (D) intramolecular FRET sensors was induced, and concentration-response curves to carbachol at the hM_3-R (C) and clozapine *N*-oxide (CNO) at the hM_3-RASSL (D) variants were constructed based on the maximal amplitude of the FRET sensor response. Data are mean ± S.E.M. from 10 to 15 individual cells.

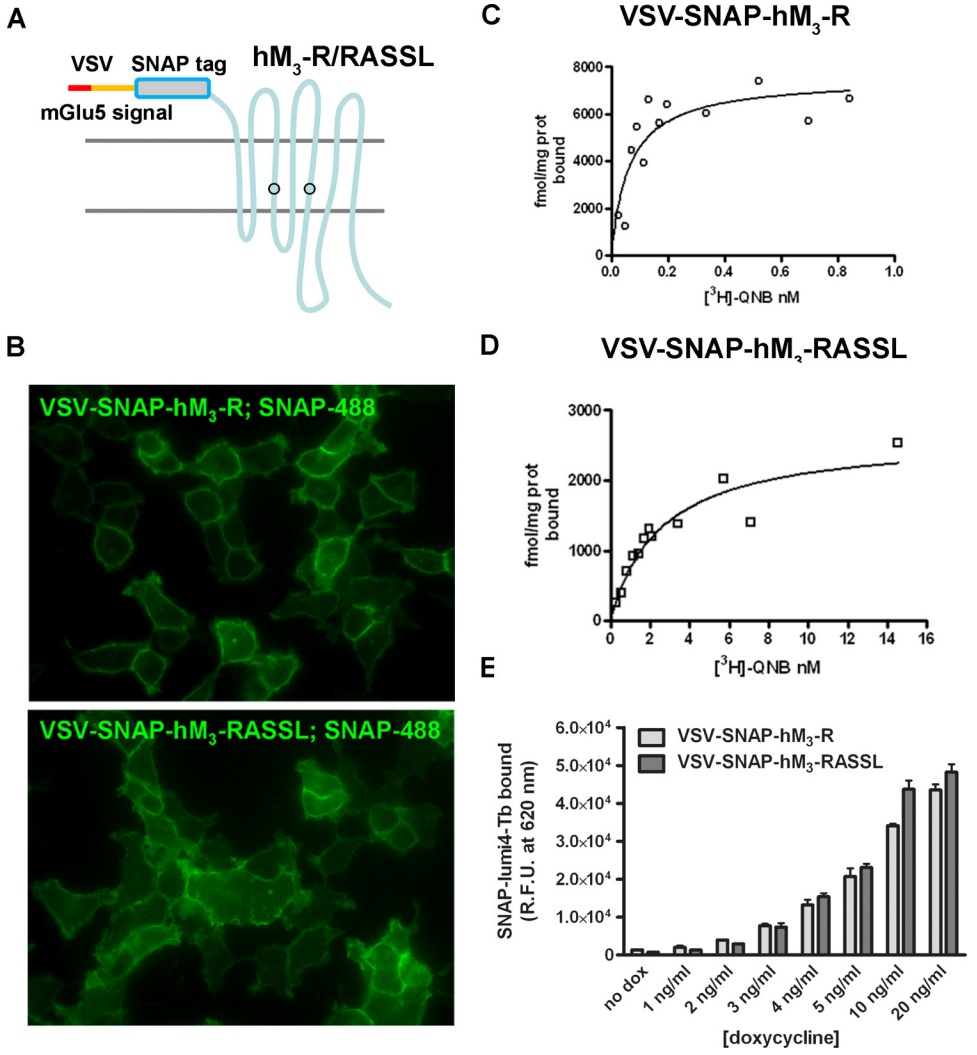

Fig. 4. Expression and detection of VSV-G- and SNAP-tagged forms of hM_3 receptor. VSV-G and SNAP-tag sequences were added at the N terminus of either hM_3-R or hM_3-RASSL. A signal sequence derived from the metabotropic glutamate receptor 5 was also included at the extreme N terminus as described previously (Alvarez-Curto et al., 2010). A diagram of the constructs is shown (A) in which the circles represent amino acids mutated to generate the RASSL variant. After the production of Flp-In T-REx 293 lines harboring either of these constructs at the inducible locus, cells maintained on glass coverslips were treated with doxycycline (5 ng/ml, 24 h) and, after addition of SNAP-488 (5 μM, 30 min), were imaged (B). Membranes prepared from cells induced to express VSV-G-SNAP hM_3-R (C) or VSV-G-SNAP hM_3-RASSL (D) were used to measure the specific binding of varying concentrations of [^{3}H]QNB. Intact cells harboring VSV-G-SNAP hM_3-R (light bars) or VSV-G-SNAP hM_3-RASSL (dark bars) were untreated (no dox) or treated with the indicated concentrations of doxycycline for 24 h. Subsequently 20 nM SNAP-lumi4Tb was added for 1 h, and after washing, luminescence intensity at 620 nm was measured after excitation at 337 nm (E). Data are means ± S.E.M. of triplicate assays from two independent experiments.

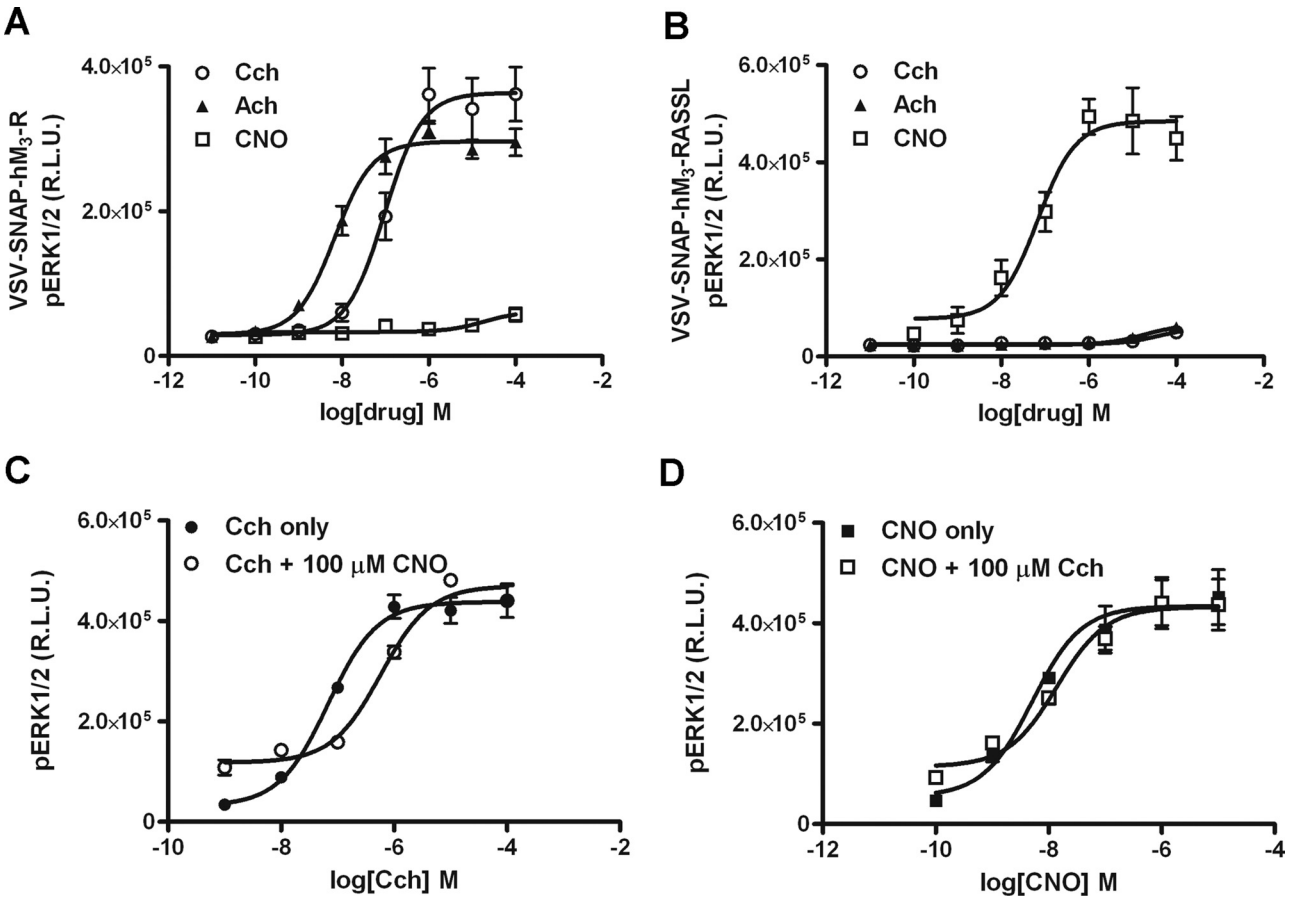

Fig. 5. Selective activation of ERK1/2 phosphorylation via VSV-G-SNAP hM_3-R or VSV-G-SNAP hM_3-RASSL. Flp-In T-REx 293 cells harboring VSV-G-SNAP hM_3-R (A and C) or VSV-G-SNAP hM_3-RASSL (B and D) were induced to express these constructs by treatment with doxycycline (5 ng/ml, 24 h). Subsequently, cells were stimulated for 5 min with varying concentrations of acetylcholine (Ach), carbachol (Cch), or clozapine *N*-oxide (CNO), and ERK1/2 phosphorylation was assessed using the AlphaScreen Surefire kit. C, the effect of varying concentrations of carbachol was assessed in the concurrent presence of 100 μM CNO. D, the effect of varying concentrations of CNO was assessed in the presence of 100 μM carbachol. Data represent means ± S.E.M. from three experiments.

Analysis of the Phosphorylation Status of hM_3-R and hM_3-RASSL. We have previously demonstrated that the M_3-receptor is phosphorylated on multiple sites in response to agonist occupation (Butcher et al., 2011). We have also presented evidence that the nature of receptor phosphorylation is influenced not only by the cell type in which the receptor is expressed but also by the ligand used to stimulate the receptor (Butcher et al., 2011). We have proposed that the difference in the profile of receptor phosphorylation seen within different cell types might represent a phosphorylation "bar code" that can direct signaling (Tobin, 2008; Tobin et al., 2008). In light of these observations, we assessed whether clozapine *N*-oxide could induce phosphorylation of the hM_3-RASSL and, if so, whether the profile of receptor phosphorylation, and therefore the phosphorylation "bar code," was comparable with that observed for hM_3-R stimulated by acetylcholine.

Metabolic labeling of Flp-In T-REx 293 cells expressing VSV-G-SNAP hM_3-R or VSV-G-SNAP hM_3-RASSL with [^{32}P]orthophosphate followed by immunoprecipitation of the receptors using a receptor-specific antibody was used to determine the receptor-phosphorylation status (Fig. 8). Using this approach, it was determined that both hM_3-R and hM_3-RASSL receptors were phosphorylated in the basal state (Fig. 8B). In these experiments, the receptor appeared as a band, running at 125 kDa in SDS-PAGE, that was present only in cells induced with doxycycline to express the receptor (Fig. 8, A and B). Consistent with the ligand binding and functional data presented above, hM_3-R showed increased phosphorylation in response to acetylcholine but showed no change in phosphorylation upon addition of clozapine *N*-oxide. In contrast, phosphorylation of VSV-G-SNAP hM_3-RASSL was increased only by clozapine *N*-oxide (Fig. 8B). To examine the pattern of phosphorylation, the immunoprecipitated receptors were partially digested with trypsin before two-dimensional resolution. This approach has been used previously to determine the pattern of muscarinic receptor phosphorylation (Torrecilla et al., 2007; Butcher et al., 2011). Here the pattern of phosphorylation of hM_3-R in response to acetylcholine was very similar to that observed for the hM_3-RASSL in response to clozapine *N*-oxide (Fig. 8C).

We further probed individual sites of phosphorylation with phosphospecific antibodies that react with pS412 within the IL3, or pS577 within the C-terminal tail (Butcher et al., 2011). Acetylcholine acting at hM_3-R and clozapine *N*-oxide acting at hM_3-RASSL increased to a similar extent the phosphorylation of sites pS412 (Fig. 9A) and pS577 (Fig. 9B). These studies indicated that the phosphorylation status of the hM_3-RASSL in response to clozapine *N*-oxide was very

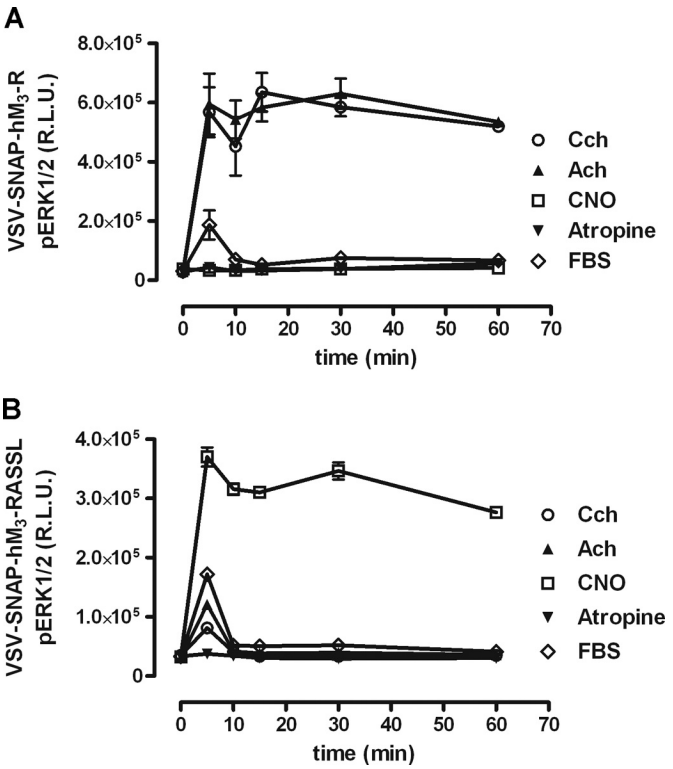

Fig. 6. Equivalent and sustained kinetics of ERK1/2 phosphorylation via VSV-G-SNAP hM_3-R or VSV-G-SNAP hM_3-RASSL. The ability of carbachol (Cch), acetylcholine (Ach), and clozapine *N*-oxide (CNO) to stimulate ERK1/2 phosphorylation was assessed at various times of exposure to ligands (all 100 μM) in cells induced to express VSV-G-SNAP hM_3-R (A) or VSV-G-SNAP hM_3-RASSL (B) as in Fig. 5. The lack of effect of atropine and a transient effect of fetal bovine serum (FBS) were also recorded in both cell lines. Data represent means ± S.E.M. from four experiments.

similar to that observed for the hM_3-R in response to the endogenous ligand acetylcholine.

The Basis for Ligand Selectivity of the RASSL. Although the results of the chemical genetic engineering are clear-cut, the molecular basis for this is less obvious. In the case of loss of potency and/or affinity for acetylcholine and carbachol (and muscarinic antagonists), the importance of Asp3.32 in providing a charge partner for the positively charged ligand is well established. Tyr3.33, located next to Asp3.32, is also postulated to make a cation-π interaction with acetylcholine and, together with Asp3.32, to keep the charge fixed in space (Grauert et al., 2010). To attempt to understand why these alterations also result in enhanced potency and/or affinity for clozapine *N*-oxide, homology models (Grauert et al., 2010; Tautermann, 2011) of the hM_3-R were generated and used initially to predict the mode of binding of clozapine, which is known to have modest affinity for hM_3-R. Here, the charged center of the piperazine moiety interacts with Asp3.32 allowing the rest of the molecule to fit within the orthosteric binding site. However, in hM_3-R, Tyr3.33 clashes with the ligand, and its replacement by cysteine in the hM_3-RASSL makes the interaction of ligand and receptor easier (Fig. 10). Furthermore, in hM_3-R, tyrosines at positions 6.51 and 7.39, along with Tyr3.33, form a roof to the aromatic pocket in which the charged part of M_3 ligands bind. In the RASSL, one side of this is absent and, hence, ligands may move slightly. This was observed when docking clozapine, in which the NH-group from the dibenzo [1,4]diazepine core interacts with Thr5.42, a residue required for activation of the M_3-R by acetylcholine (Wess et al., 1992). The A5.46G mutation makes further space for clozapine to interact with Thr5.42. It is important to note for validation of the model, therefore, that clozapine has been reported to be

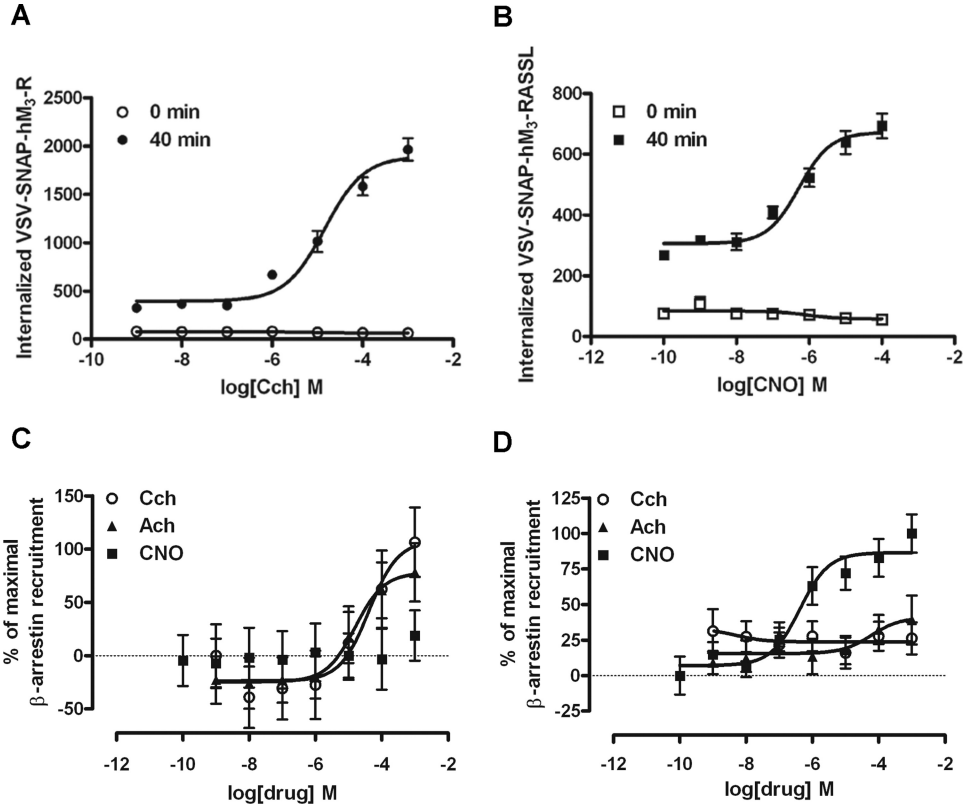

Fig. 7. Appropriate agonists promote internalization of variants of the hM_3 receptor and interactions of the receptors with β-arrestin-2. VSV-G-and SNAP-tagged hM_3-R- and hM_3-RASSL-expressing cells were labeled with 100 nM SNAP-Lumi4-Tb, a luminescent probe, and subsequently incubated with a mixture of Tag-lite internalization reagent and carbachol (Cch) or clozapine *N*-oxide (CNO) for 0 or 40 min (A and B). HEK293T cells were transiently cotransfected with β-arrestin-2-RLuc luciferase 8 and either Flag-hM_3-Citrine (C) or c-Myc-hM_3-RASSL-Citrine (D). After addition of varying concentrations of Ach, Cch, or CNO for 10 min, coelenterazine-h was added and BRET was measured as a surrogate for the recruitment of β-arrestin-2 to the forms of the hM_3 receptor. Data are means ± S.E.M. from three or four independent experiments performed in triplicate.

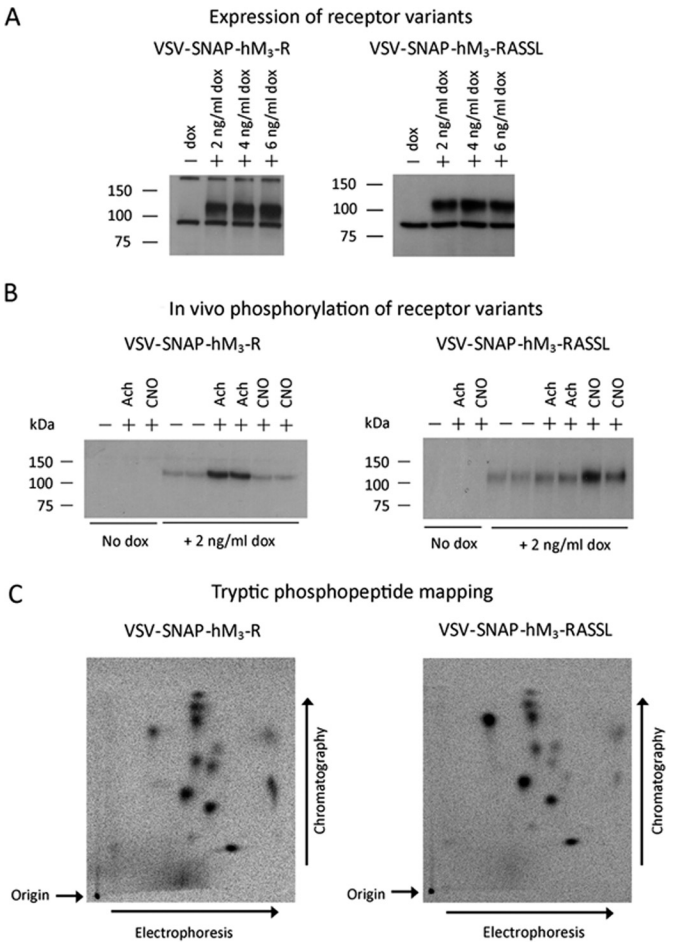

Fig. 8. Appropriate agonists regulate similar patterns of phosphorylation on the hM_3 receptor variants. Flp-In T-REx 293 cells harboring VSV-G-SNAP hM_3-R (A, left) or VSV-G-SNAP hM_3-RASSL (A, right) were uninduced (no dox) or induced to express these constructs by treatment with doxycycline (2 ng/ml, 24 h). Lysates from these cells were resolved by SDS-PAGE and immunoblotted with an anti-M_3 receptor antiserum. B and C, cells as in A were labeled with $^{32}P_i$ and subsequently challenged with acetylcholine (ACH) or clozapine *N*-oxide (CNO) for 5 min. Lysates from these cells were immunoprecipitated with the anti-M_3 receptor antiserum and resolved by SDS-PAGE (B) or after limited tryptic digestion, two-dimensional peptide mapping (C). The figures are representative of results produced in four independent experiments.

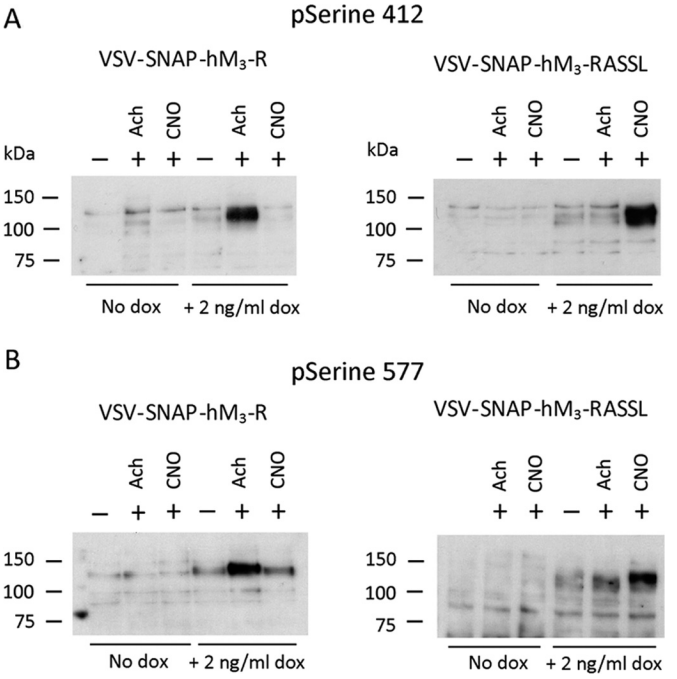

Fig. 9. Appropriate agonists modulate phosphorylation of specific residues in hM_3 receptor variants equivalently. Flp-In T-REx 293 cells harboring VSV-G-SNAP hM_3-R (left) or VSV-G-SNAP hM_3-RASSL (right) were uninduced (no dox) or induced to express these constructs by treatment with doxycycline (2 ng/ml, 24 h). After addition of acetylcholine (Ach) or clozapine *N*-oxide (CNO) for 5 min, cell lysates were generated and resolved by SDS-PAGE and immunoblotted with phospho-specific antibodies able to identify phospho-serine 412 (A) or phospho-serine 577 (B). Data are representative of results produced in three independent experiments.

100-fold more potent in Ca^{2+} assays at the hM_3-RASSL than at hM_3-R (Armbruster et al., 2007). It is noteworthy that clozapine *N*-oxide does not fit well into the binding site of hM_3-R because it lacks the positively charged head-group to interact with D3.32, explaining its lack of potency/affinity at the wild type and the inability to compete with carbachol/acetylcholine as shown in Fig. 5. However, on the basis that it would be likely to dock into hM_3-R in a similar orientation as clozapine, interactions in the aromatic/Asp3.32 cage are poor with the piperazine-*N*-oxide group, therefore the ligand moves slightly away from Asp3.32, causing the opening of the roof of the binding pocket (i.e., the network of tyrosines 3.33, 6.51, and 7.39 is interrupted) and upward movement (Fig. 10). Thus, even if clozapine *N*-oxide were able to bind with low affinity to hM_3-R (and the data of Fig. 5 indicate any such affinity to be very low) no interaction could be formed with Thr5.42, and thus no agonist action would be expected. In contrast, for hM_3-RASSL, the roof of the aromatic cage binding site does not exist and clozapine *N*-oxide thus does not need to break this energetically favorable interaction. The piperazine-*N*-oxide interacts with the aromatic cage (the N is closer to Asp3.32 and the O is close to Cys7.42—possibly allowing a hydrogen bond interaction), and the aromatic part of the molecule moves toward transmembrane domain 5, interacting with Thr5.42 (Fig. 10). Also, the mutation A5.46G allows clozapine *N*-oxide to come closer to and interact with Thr5.42. As noted previously (Alvarez-Curto et al., 2010), the affinity of hM_3-RASSL constructs to bind muscarinic antagonists, including [^{3}H]QNB and atropine, was significantly lower than the hM_3-R forms. This was not unexpected, because these ligands interact with many of the same residues as acetylcholine and are competitive with the endogenous ligand.

Discussion

Our study is the first to comprehensively test whether synthetic ligands acting at a RASSL receptor are able to mediate receptor responses that are similar to those of the natural ligand operating at the wild-type receptor. Such analysis is critical in validation of the use of RASSL receptors in transgenic studies designed to test the function of GPCRs and in the use of such RASSLs in defining selective GPCRs as therapeutic targets. Recent studies that have determined that different GPCR ligands can stabilize or induce different conformations of a receptor and that these can differentially engage G protein subtypes and other downstream signaling proteins in a process called functional selectivity or ligand bias raise the very real possibility that synthetic ligands

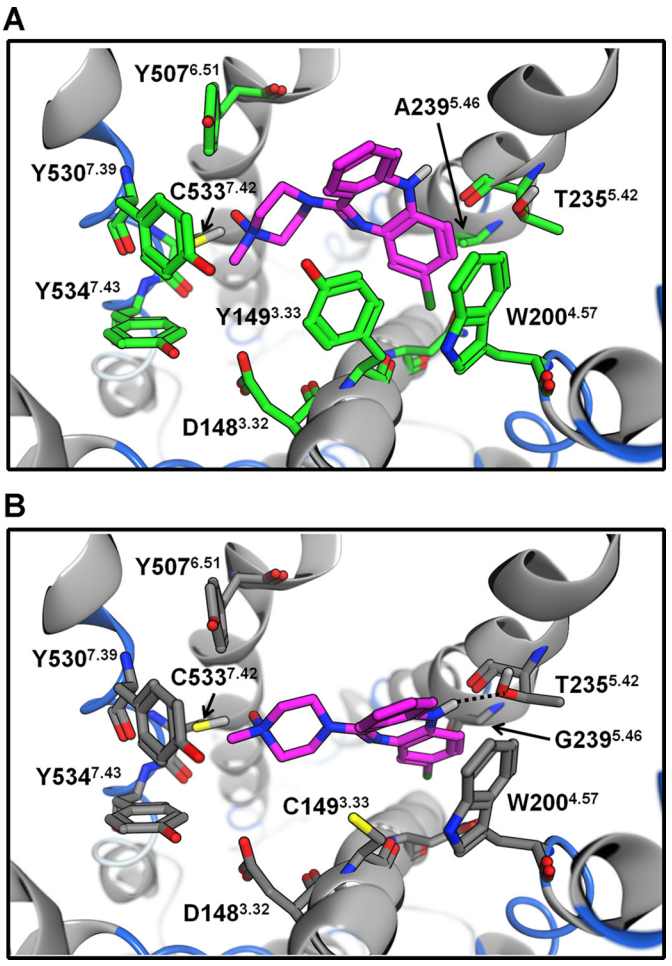

Fig. 10. The basis of selective interactions of clozapine *N*-oxide with hM_3-RASSL. The proposed binding mode of clozapine *N*-oxide (pink) to hM_3-R (A) and to the hM_3-RASSL (B). Mutation of Tyr3.33 (hM_3-R) to Cys3.33 (hM_3-RASSL) allows clozapine *N*-oxide to move in the binding site and to interact with Thr5.42 (H-bond depicted as dotted line). Residues within the binding site predicted to play important roles are denoted both as their position in the primary sequence of hM_3-R and by their relative positions within transmembrane helices as described by Ballesteros and Weinstein (1995).

acting on RASSL receptors might show bias that will result in a different signaling profile of the RASSL receptor from the wild type. Given this possibility and the huge experimental potential of RASSL receptors, it would seem essential that careful characterization of the signaling properties of such receptor mutants must be addressed.

We approach this question here by using a RASSL of the hM_3-muscarinic receptor that was developed on the basis that the drug clozapine has relatively low affinity/potency at muscarinic receptor subtypes and the related molecule clozapine *N*-oxide is essentially inactive. Armbruster et al. (2007) hence scanned randomly generated point mutants of the M_3-receptor for loss of potency to acetylcholine and a concurrent gain of potency to clozapine *N*-oxide. They noted that by combining two point mutants in the M_3 receptor, cysteine for tyrosine at position 3.33 and glycine for alanine at position 5.46 (Armbruster et al., 2007), a large alteration in the potency ratio in favor of clozapine *N*-oxide over acetylcholine was achieved. Moreover, because the amino acids at positions 3.33 and 5.46 are conserved in the other 4 muscarinic receptor subtypes, the same alterations result in similar changes in pharmacology (Armbruster et al., 2007). In the various approaches used herein, it would be anticipated that the potency of ligands in the intramolecular FRET studies and in both the internalization and β-arrestin-2 interaction studies should provide reasonable surrogate estimates of agonist affinity, because each of these is linked closely to receptor occupancy. By contrast, signals measured downstream (i.e., elevation of intracellular Ca^{2+} and ERK1/2 MAP kinase phosphorylation) involve amplification and therefore the presence of receptor reserve accounts for the lower concentrations of ligands required to produce half-maximal effects. Indeed, the results from the assays linked closely to receptor occupancy indicate that acetylcholine has affinity estimated in the region of 10 μM for the various forms of hM_3-R used, whereas clozapine *N*-oxide has affinity estimated as close to 1 μM for the hM_3-RASSL forms (Table 1).

Functionality of agonist ligands can be assessed at many levels within signal transduction cascades, and we employed a wide range of assays to define the equivalence (or otherwise) of action of acetylcholine at hM_3-R and clozapine *N*-oxide at the hM_3-RASSL variants. Initial conformational changes of receptors upon binding of an agonist can be monitored by intramolecular FRET studies if appropriate FRET donor and acceptor species are integrated into sites within the receptor that move or reorient relative to one another upon agonist binding. Because observations from agonist-bound atomic-level structures of GPCRs (Rosenbaum et al., 2011; Xu et al., 2011) have supported earlier predictions about outward movement of the intracellular end of transmembrane domain 6, then alterations in FRET signal within a receptor are anticipated if a FRET acceptor is placed in the third intracellular loop, because this links transmembrane domains 5 and 6, and a FRET donor is linked to the C-terminal tail of the receptor (Hoffmann et al., 2005; Zürn et al., 2009). Such an intramolecular FRET sensor has been validated previously for the hM_3-R (Ziegler et al., 2011). In initial studies, we introduced both Y3.33C and A5.46G mutations to produce the hM_3-RASSL and also assessed the effect on response to both clozapine *N*-oxide and acetylcholine/carbachol on equivalent sensors expressing either mutation in isolation. Because these studies validated the anticipated responsiveness of the sensors, we generated stably transfected cell lines able to express either the hM_3-R or hM_3-RASSL sensor and used them to generate concentration response data.

Although some aspects of signal generation of the hM_3-RASSL and comparisons with the wild-type receptor have been assessed previously (Armbruster et al., 2007) as a prelude to generation of transgenic animals expressing this variant, these were very limited in scope and were performed before recent studies that have determined that subtle variation in receptor conformation (mediated by receptor mutations or the binding of different ligands) can have a profound impact on the signaling outcomes of a receptor. These earlier studies also did not fully appreciate our developing understanding of biased signaling and functional selectivity—all of which are potential mechanisms by which RASSL receptors might mediate distinct signal profiles from that of wild-type receptors. This means that, in retrospect, the initial studies (Armbruster et al., 2007) were too superficial to conclude that such RASSL receptors signal in a manner equivalent to that of the wild-type receptors.

We have previously used cell lines able to express versions of the hM_3-R and hM_3-RASSL, modified to incorporate SNAP-tags in their extracellular N-terminal domain, to employ time-resolved FRET studies based on Tag-lite reagents to explore the quaternary organization of cell surface hM_3 receptors (Alvarez-Curto et al., 2010). Internalization of each form of hM_3 was produced only in response to the anticipated ligands and, at maximally effective ligand concentration, was of similar extent. Likewise, hM_3-R and hM_3-RASSL variants were able to interact with β-arrestin-2 only in response to the appropriate agonists and in a ligand concentration-dependent manner. Integrated measures of downstream signal transduction were also compared by assessing phosphorylation of the ERK1/2 MAP kinases. In both cases, this effect was extensive and was maintained for a prolonged period. There was no indication of differences in levels of constitutive activity between the hM_3-R and hM_3-RASSL, because ERK1/2 phosphorylation in the absence of agonist ligands was not different. In contrast to activation of the forms of hM_3, ERK1/2 phosphorylation promoted by FBS in each cell line was transitory in nature, returning to basal levels within a 15-min period. Transient ERK1/2 phosphorylation was also noted to both acetylcholine and carbachol in cells expressing hM_3-RASSL. Although we have not explored this in detail, it is likely to reflect the known endogenous expression of low levels of hM_3-R in HEK293-derived cells (Shaw et al., 2002), whereas activation of the endogenous receptor in cells expressing the hM_3-R sensor is presumably masked by the large response generated by the sensor.

A key assessment of the likely equivalence of activation of hM_3-R by acetylcholine and hM_3-RASSL by clozapine *N*-oxide was performed in studies that assessed the extent of phosphorylation of the receptor variants after addition of agonists. Analysis of either the global pattern of phosphorylation using tryptic phospho-peptide maps or analysis of individual sites of phosphorylation using receptor phospho-specific antibodies showed there to be no significance difference in the phosphorylation profile of the wild-type hM_3-R and the hM_3-RASSL mutant.

This is important in light of studies indicating that the pattern of receptor phosphorylation can contribute to the signaling outcome of the receptor (Poulin et al., 2010 Tobin et al., 2008). Thus, if the phosphorylation pattern, or phosphorylation "bar code," between the hM_3-RASSL and hM_3-R were different, then this might suggest that the signaling of the two receptors might be different. The fact that the phosphorylation pattern was equivalent between the receptor variants after agonist stimulation would point to the likelihood of the signaling outcomes of these receptors being equivalent. This conclusion is consistent with the fact that we show here that ERK-1/2 activation, β-arrestin recruitment, and receptor internalization of the hM_3-RASSL and hM_3-R after stimulation with clozapine-*N*-oxide and acetylcholine, respectively, was similar.

Our studies, therefore, indicate that the response of the hM_3-RASSL to clozapine-*N*-oxide is very similar to that of the hM_3-R to acetylcholine. This is important because analysis of the binding characteristics of clozapine-*N*-oxide carried out here indicates that the mechanism of receptor activation of the hM_3-RASSL is subtly different from that of acetylcholine activation of hM_3-R. Given that there is now accumulating evidence that different orthosteric ligands to GPCRs can drive different signaling outcomes in a process called ligand bias or functional selectively (Mailman, 2007; Kenakin, 2011; Smith et al., 2011), the subtle differences in the activation mechanism of the hM_3-RASSL and hM_3-R might manifest itself in differences in the signaling properties of these receptor variants. The detailed analysis carried out here indicates that there is no functional selectivity associated with clozapine-*N*-oxide at the hM_3-RASSL. This validates the use of this particular RASSL receptor mutant in transgenic studies of receptor action where the pharmacological stimulation of the hM_3-RASSL expressed in a genetically engineered mouse strain is presumed to mimic the actions of the wild type hM_3-R. In light of our study, we can view with confidence the data generated from the hM_3-RASSL receptor in neuronal (Alexander et al., 2009) and pancreatic studies (Guettier et al., 2009) and pursue future transgenic studies in our own laboratory aimed at conditionally expressing the hM_3-RASSL in place of the wild-type hM_3-R. Despite these results, the ongoing production of novel RASSLs from different parental receptors cautions that studies equivalent to these must be performed routinely as a prelude to their in vivo expression and analysis of function.

Authorship Contributions

Participated in research design: Alvarez-Curto, Tobin, and Milligan.

Conducted experiments: Alvarez-Curto, Prihandoko, Tautermann, and Pediani.

Contributed new reagents or analytical tools: Zwier, Lohse, Hoffmann, and Tobin.

Performed data analysis: Alvarez-Curto, Prihandoko, Tautermann, Pediani, Tobin, and Milligan.

Wrote or contributed to the writing of the manuscript: Alvarez-Curto, Prihandoko, Tautermann, Zwier, Pediani, Lohse, Hoffmann, Tobin, and Milligan.

References

Alexander GM, Rogan SC, Abbas AI, Armbruster BN, Pei Y, Allen JA, Nonneman RJ, Hartmann J, Moy SS, Nicolelis MA, et al. (2009) Remote control of neuronal activity in transgenic mice expressing evolved G protein-coupled receptors. *Neuron* **63:**27–39.

Alvarez-Curto E, Ward RJ, Pediani JD, and Milligan G (2010) Ligand regulation of the quaternary organization of cell surface M3 muscarinic acetylcholine receptors analyzed by fluorescence resonance energy transfer (FRET) imaging and homogeneous time-resolved FRET. *J Biol Chem* **285:**23318–23330.

Armbruster BN, Li X, Pausch MH, Herlitze S, and Roth BL (2007) Evolving the lock to fit the key to create a family of G protein-coupled receptors potently activated by an inert ligand. *Proc Natl Acad Sci USA* **104:**5163–5168.

Ballesteros JA and Weinstein H (1995) Integrated methods for the construction of three dimensional models and computational probing of structure-function relations in G-protein coupled receptors. *Methods Neurosci* **25:**366–428.

Bhattacharya S, Hall SE, Li H, and Vaidehi N (2008) Ligand-stabilized conformational states of human beta(2) adrenergic receptor: insight into G-protein-coupled receptor activation. *Biophys J* **94:**2027–2042.

Butcher AJ, Prihandoko R, Kong KC, McWilliams P, Edwards JM, Bottrill A, Mistry S, and Tobin AB (2011) Differential G-protein-coupled receptor phosphorylation provides evidence for a signaling bar code. *J Biol Chem* **286:**11506–11518.

Chang WC, Ng JK, Nguyen T, Pellissier L, Claeysen S, Hsiao EC, and Conklin BR (2007) Modifying ligand-induced and constitutive signaling of the human 5-HT4 receptor. *PLoS One* **2:**e1317.

Conklin BR, Hsiao EC, Claeysen S, Dumuis A, Srinivasan S, Forsayeth JR, Guettier JM, Chang WC, Pei Y, McCarthy K_D, et al. (2008) Engineering GPCR signaling pathways with RASSLs. *Nat Methods* **5:**673–678.

Conn PJ, Jones CK, and Lindsley CW (2009) Subtype-selective allosteric modulators of muscarinic receptors for the treatment of CNS disorders. *Trends Pharmacol Sci* **30:**148–155.

Digby GJ, Shirey JK, and Conn PJ (2010) Allosteric activators of muscarinic receptors as novel approaches for treatment of CNS disorders. *Mol Biosyst* **6:**1345–1354.

Dong S, Rogan SC, and Roth BL (2010) Directed molecular evolution of DREADDs: a generic approach to creating next-generation RASSLs. *Nat Protoc* **5:**561–573.

Ellis J, Pediani JD, Canals M, Milasta S, and Milligan G (2006) Orexin-1 receptor-cannabinoid CB1 receptor heterodimerization results in both ligand-dependent and -independent coordinated alterations of receptor localization and function. *J Biol Chem* **281:**38812–38824.

Gautier A, Juillerat A, Heinis C, Corrêa IR Jr, Kindermann M, Beaufils F, and

Johnsson K (2008) An engineered protein tag for multiprotein labeling in living cells. *Chem Biol* **15:**128–136.
Grauert M, Pieper MP, and Casarosa P (2010) Muscarinic receptor antagonists in the treatment of COPD, in *Analogue-Based Drug Discovery II* (Fischer J and Ganellin CR eds) pp 297–318, WILEY-VCH Verlag GmbH & Co. KGaA, Weinheim, Germany.
Guettier JM, Gautam D, Scarselli M, Ruiz de Azua I, Li JH, Rosemond E, Ma X, Gonzalez FJ, Armbruster BN, Lu H, et al. (2009) A chemical-genetic approach to study G protein regulation of beta cell function in vivo. *Proc Natl Acad Sci USA* **106:**19197–19202.
Hoffmann C, Gaietta G, Bünemann M, Adams SR, Oberdorff-Maass S, Behr B, Vilardaga JP, Tsien RY, Ellisman MH, and Lohse MJ (2005) A FlAsH-based FRET approach to determine G protein-coupled receptor activation in living cells. *Nat Methods* **2:**171–176.
Jenkins L, Alvarez-Curto E, Campbell K, de Munnik S, Canals M, Schlyer S, and Milligan G (2011) Agonist activation of the G protein-coupled receptor GPR35 involves transmembrane domain III and is transduced via Galpha13 and beta-arrestin-2. *Br J Pharmacol* **162:**733–748.
Jenkins L, Brea J, Smith NJ, Hudson BD, Reilly G, Bryant NJ, Castro M, Loza MI, and Milligan G (2010) Identification of novel species-selective agonists of the G-protein-coupled receptor GPR35 that promote recruitment of beta-arrestin-2 and activate Galpha13. *Biochem J* **432:**451–459.
Kenakin T (2011) Functional selectivity and biased receptor signaling. *J Pharmacol Exp Ther* **336:**296–302.
Kobilka BK and Deupi X (2007) Conformational complexity of G-protein-coupled receptors. *Trends Pharmacol Sci* **28:**397–406.
Mailman RB (2007) GPCR functional selectivity has therapeutic impact. *Trends Pharmacol Sci* **28:**390–396.
Nawaratne V, Leach K, Suratman N, Loiacono RE, Felder CC, Armbruster BN, Roth BL, Sexton PM, and Christopoulos A (2008) New insights into the function of M4 muscarinic acetylcholine receptors gained using a novel allosteric modulator and a DREADD (designer receptor exclusively activated by a designer drug). *Mol Pharmacol* **74:**1119–1131.
Pei Y, Rogan SC, Yan F, and Roth BL (2008) Engineered GPCRs as tools to modulate signal transduction. *Physiology* **23:**313–321.
Poulin B, Butcher A, McWilliams P, Bourgognon JM, Pawlak R, Kong KC, Bottrill A, Mistry S, Wess J, Rosethorne EM, et al. (2010) The M3-muscarinic receptor regulates learning and memory in a receptor phosphorylation/arrestin-dependent manner. *Proc Natl Acad Sci USA* **107:**9440–9445.
Rajagopal S, Rajagopal K, and Lefkowitz RJ (2010) Teaching old receptors new tricks: biasing seven-transmembrane receptors. *Nat Rev Drug Discov* **9:**373–386.
Redfern CH, Coward P, Degtyarev MY, Lee EK, Kwa AT, Hennighausen L, Bujard H, Fishman GI, and Conklin BR (1999) Conditional expression and signaling of a specifically designed Gi-coupled receptor in transgenic mice. *Nat Biotechnol* **17:**165–169.
Rosenbaum DM, Zhang C, Lyons JA, Holl R, Aragao D, Arlow DH, Rasmussen SG, Choi HJ, Devree BT, Sunahara RK, et al. (2011) Structure and function of an irreversible agonist-beta(2) adrenoceptor complex. *Nature* **469:**236–240.
Shaw G, Morse S, Ararat M, and Graham FL (2002) Preferential transformation of human neuronal cells by human adenoviruses and the origin of HEK 293 cells. *FASEB J* **16:**869–871.
Smith NJ, Bennett KA, and Milligan G (2011) When simple agonism is not enough: emerging modalities of GPCR ligands. *Mol Cell Endocrinol* **331:**241–247.
Smith NJ, Stoddart LA, Devine NM, Jenkins L, and Milligan G (2009) The action and mode of binding of thiazolidinedione ligands at free fatty acid receptor 1. *J Biol Chem* **284:**17527–17539.
Stoddart LA, Smith NJ, Jenkins L, Brown AJ, and Milligan G (2008) Conserved polar residues in transmembrane domains V, VI, and VII of free fatty acid receptor 2 and free fatty acid receptor 3 are required for the binding and function of short chain fatty acids. *J Biol Chem* **283:**32913–32924.
Swaminath G, Deupi X, Lee TW, Zhu W, Thian FS, Kobilka TS, and Kobilka B (2005) Probing the beta2 adrenoceptor binding site with catechol reveals differences in binding and activation by agonists and partial agonists. *J Biol Chem* **280:**22165–22171.
Sweger EJ, Casper KB, Scearce-Levie K, Conklin BR, and McCarthy K_D (2007) Development of hydrocephalus in mice expressing the G(i)-coupled GPCR Ro1 RASSL receptor in astrocytes. *J Neurosci* **27:**2309–2317.
Tautermann CS (2011) The use of G-protein coupled receptor models in lead optimization. *Future Med Chem* **3:**709–721.
Tobin AB (2008) G-protein-coupled receptor phosphorylation: where, when and by whom. *Br J Pharmacol* **153 (Suppl 1):**S167–S176.
Tobin AB, Butcher AJ, and Kong KC (2008) Location, location, location… site-specific GPCR phosphorylation offers a mechanism for cell-type-specific signalling. *Trends Pharmacol Sci* **29:**413–420.
Torrecilla I, Spragg EJ, Poulin B, McWilliams PJ, Mistry SC, Blaukat A, and Tobin AB (2007) Phosphorylation and regulation of a G protein-coupled receptor by protein kinase CK2. *J Cell Biol* **177:**127–137.
Vaidehi N and Kenakin T (2010) The role of conformational ensembles of seven transmembrane receptors in functional selectivity. *Curr Opin Pharmacol* **10:**775–781.
Violin JD and Lefkowitz RJ (2007) Beta-arrestin-biased ligands at seven-transmembrane receptors. *Trends Pharmacol Sci* **28:**416–422.
Ward RJ, Pediani JD, and Milligan G (2011) Ligand-induced internalization of the orexin OX(1) and cannabinoid CB(1) receptors assessed via N-terminal SNAP and CLIP-tagging. *Br J Pharmacol* **162:**1439–1452.
Wess J (2004) Muscarinic acetylcholine receptor knockout mice: novel phenotypes and clinical implications. *Annu Rev Pharmacol Toxicol* **44:**423–450.
Wess J, Eglen RM, and Gautam D (2007) Muscarinic acetylcholine receptors: mutant mice provide new insights for drug development. *Nat Rev Drug Discov* **6:**721–733.
Wess J, Maggio R, Palmer JR, and Vogel Z (1992) Role of conserved threonine and tyrosine residues in acetylcholine binding and muscarinic receptor activation. A study with m3 muscarinic receptor point mutants. *J Biol Chem* **267:**19313–19319.
Xu F, Wu H, Katritch V, Han GW, Jacobson KA, Gao ZG, Cherezov V, and Stevens RC (2011) Structure of an agonist-bound human A2A adenosine receptor. *Science* **332:**322–327.
Ziegler N, Bätz J, Zabel U, Lohse MJ, and Hoffmann C (2011) FRET-based sensors for the human M1-, M3-, and M5-acetylcholine receptors. *Bioorg Med Chem* **19:**1048–1054.
Zürn A, Zabel U, Vilardaga JP, Schindelin H, Lohse MJ, and Hoffmann C (2009) Fluorescence resonance energy transfer analysis of alpha 2a-adrenergic receptor activation reveals distinct agonist-specific conformational changes. *Mol Pharmacol* **75:**534–541.

Address correspondence to: Graeme Milligan, Wolfson Link Building 253, University of Glasgow, Glasgow G12 8QQ, Scotland, UK, E-mail: graeme.milligan@glasgow.ac.uk